Correlated Electric Field and Low-Energy Electron Measurements in the Low-Altitude Polar Cusp

P. M. KINTNER,[1] K. L. ACKERSON, D. A. GURNETT, AND L. A. FRANK

Department of Physics and Astronomy, University of Iowa, Iowa City, Iowa 52242

Correlated electric field and low-energy electron measurements are presented for two passes of Hawkeye 1 through the south polar cusp at 2000-km altitude during local morning. In one case the electric field reversal coincides with the boundary of detectable 5.2-keV electron intensities and the equatorward boundary of the cusp. In the other case the electric field reversal and the 5.2-keV electron trapping boundary coincide, but the equatorward edge of the cusp as determined from the presence of 180-eV electron intensities is 5° invariant latitude equatorward of the electric field reversal. We conclude that in the second case, electron intensities associated with the polar cusp populate closed dayside field lines, and hence the corresponding equatorward edge of these electron intensities is not always an indicator of the boundary between closed dayside field lines and polar cap field lines.

INTRODUCTION

The entry of magnetosheath plasma on dayside field lines just poleward of the trapping boundary and its penetration down to the ionosphere have been established at high altitudes by *Frank* [1971] and *Russell et al.* [1971] and at low altitudes by *Frank and Ackerson* [1971], *Heikkila and Winningham* [1971], and *Maynard and Johnstone* [1974]. Since the cusp marks the transition from dayside field lines to polar cap field lines, the polar cusp and its ionospheric projection, the midday aurora [*Heikkila et al.*, 1972], have been used to infer changes in the earth's magnetic field configuration [*Akasofu*, 1972*a*, *b*; *Yasuhara et al.*, 1973; *Kivelson et al.*, 1973]. Similarly, the flow of low-altitude thermal plasma at high latitudes is the projection of the earth's magnetic field line motion at high altitudes and is also responsive to the configuration of the magnetosphere. Low-altitude measurements of electric fields by satellite-borne double probes [*Cauffman and Gurnett*, 1971; *Heppner*, 1972*a*] and by barium clouds [*Wescott et al.*, 1969] have established that the high-latitude plasma convection generally consists of antisunward flow over the polar cap, an abrupt reversal in the east-west direction of flow at the equatorward boundary of the polar cap, and a sunward flow equatorward of the reversal. The flow speed generally peaks near the reversal. Simultaneous plasma and electric field measurements on the dayside of the polar cap, near the polar cusp, were first presented by *Gurnett and Frank* [1973], using data from the Injun 5 satellite. They found that the convection reversal occurred near the low-latitude boundary of the cusp plasma, although there was considerable uncertainty in the exact relationship, since the spatial resolution of the measurements was comparable to the width of the polar cusp. *Heelis et al.* [1976], using ion drift detectors, have obtained vector measurements of the convection velocity over the polar cap. Their measurements confirm the existence of abrupt velocity reversal on the flanks of the polar cap. However, they also showed that near noon the flow in the polar cusp is antisunward, and instead of reversing the velocity field rotates so that the component of flow normal to the low-latitude boundary of the polar cap is finite across the boundary. Substantial dawn-dusk components to the plasma flow were also observed near the polar cusp.

This paper presents simultaneous electric field and plasma measurements from the Hawkeye 1 satellite at low altitudes over the southern polar cap. The primary objective of this study is to further investigate the relationship of the plasma flow to the spatial structure of the polar cusp plasma distribution by using the improved spatial resolution of the Hawkeye 1 measurements compared to the earlier Injun 5 results.

INSTRUMENTATION

Hawkeye 1 was launched on June 3, 1974, into an elliptical orbit with an apogee of 21 R_E over the northern polar cap and a perigee of 1800 km over the southern polar cap. The instrumentation on board consists of a complement of magnetic field, electric field, and particle detectors designed to study the properties of the polar cusp.

The electric field antenna is a copper-beryllium cylinder with a tip-to-tip length of 42.45 m and a diameter of 0.67 cm. The inner 30.2 m of antenna are insulated, leaving two exposed probes of 6.1-m length at each end. Static electric fields parallel to the antenna are obtained by measuring the difference in the floating potential of each probe, using a voltmeter with an input impedance of 10^{10} Ω. To determine the electric field in a fixed frame of reference, the $\mathbf{v} \times \mathbf{B}$ potential resulting from the spacecraft's motion through the earth's magnetic field must be subtracted from the electric field measured in the spacecraft frame of reference. Corrections for slow changes in the effective antenna length are also included. At high altitudes over the northern polar cap, photoelectrons of spacecraft origin substantially modified the ambient static electric field. Consequently, the electric field data reported here were measured while the satellite was at low altitudes over the southern polar cap.

Since Hawkeye 1 is spinning with the electric antenna axis oriented perpendicular to the spin axis, the measured antenna potential difference is a sinusoid in time. The spin period is 11.009 s. Approximately 12 samples of the potential difference between the two probes are telemetered each spin. A sinusoidal least mean squares fit is made to the 12 samples to obtain the phase and amplitude of the signal. Because of a failure of the attitude determination system about 3 months after launch the absolute orientation is determined by comparing the on-board magnetic field with a theoretical model of the earth's magnetic field. Figure 1 indicates the reference system used to analyze the signal and to infer the electric field in three dimensions. The z axis is the spacecraft spin axis. The

[1]Now at the School of Electrical Engineering, Cornell University, Ithaca, New York 14850.

Paper number 7A0574.
0148-0227/78/017A-0574$03.00

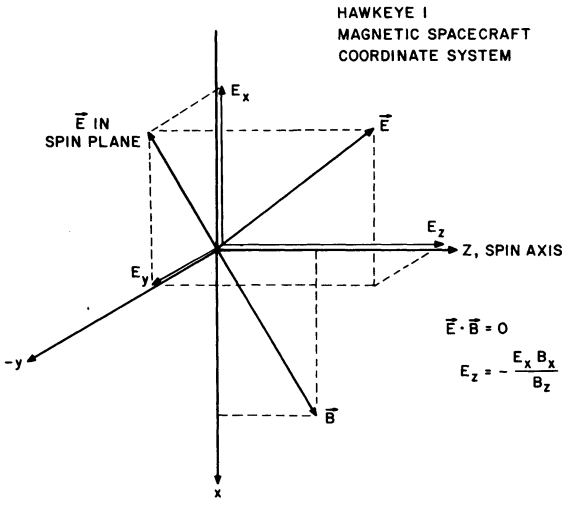

Fig. 1. The reference frame for calculating the vector electric field in the plane perpendicular to the local magnetic field. The projection of the local magnetic field onto the spin plane is defined as the x axis.

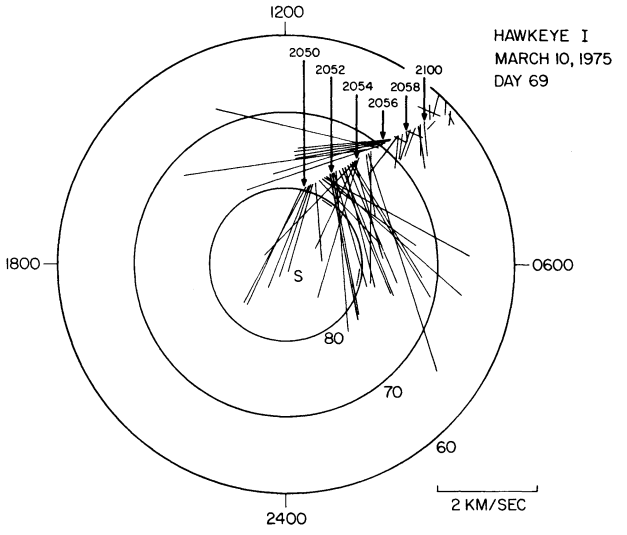

Fig. 2. The **E** × **B** velocities plotted once each spacecraft spin from the spacecraft position in invariant latitude and magnetic local time for March 10, 1975.

x axis is the projection of the earth's magnetic field onto the spin plane as measured by the on-board magnetometer. The electric field measured is the projection of the electric field vector onto the spin plane of the antenna. The phase of the sinusoid is referenced to the x axis so that the E_x and E_y components are calculated from the sinusoidal fit once each spin. The component E_z is calculated assuming that there are no electric fields parallel to the local magnetic field. From the relation $\mathbf{E}\cdot\mathbf{B} = 0$ with $B_y = 0$ it is seen that E_z is given by $-E_xB_x/B_z$. Once the spin axis direction is known, the total electric vector is transformed into an earth-fixed frame of reference by assuming that the measured magnetic field is in the same direction as the reference field [*Cain and Langel*, 1968]. When the magnetic field is nearly parallel to the spin axis, the coordinate system orientation is susceptible to small errors in the measured magnetic field. For this reason, situations where the magnetic field is within 15° of the spin axis have been eliminated from consideration.

The particle detectors on Hawkeye 1 consist of a Lepedea (Low-Energy Proton-Electron Differential Energy Analyzer) that measures the directional differential intensities of electrons and protons from 50 eV to 50 keV in directions perpendicular to the spacecraft spin axis and a thin-windowed Geiger-Mueller tube that responds primarily to electrons with energy greater than 45 keV. In the Ramp mode a complete electron and proton spectrum is made every 11.5 s over the energy range 100 eV to 30 keV. The Hawkeye spin axis is nearly parallel to the ecliptic plane, and consequently, the Lepedea samples a pitch angle range of up to 120° over the southern auroral zone.

Over the south polar cap the telemetry signal from Hawkeye 1 is received at Orroral, Australia. This limits the coverage to a maximum invariant latitude of −83°. The high-latitude termination of the data presented herein is the result of Hawkeye passing below the horizon for telemetry reception at Orroral.

OBSERVATIONS

The convection velocities measured along the Hawkeye 1 orbit on day 69, March 10, 1975, are shown in Figure 2 projected as viewed looking along the magnetic field vector. The velocity vector, calculated from $\mathbf{E}\times\mathbf{B}/B^2$ in an inertial frame of reference, is plotted once per spin. The lines representing the velocity vector are plotted outward from the satellite position in magnetic local time and invariant latitude. Uncertainties and variations in the effective length of the antenna limit the instrument accuracy to about 0.5 km/s. For this pass, telemetry coverage begins at 2050 UT, and the spacecraft travels from about 79° INV and 1100 hours MLT to 60° INV and 0900 hours MLT. Two zones of intense convection are present during this period. From 79° INV to 71° INV the velocity vectors have a primarily antisunward direction with peak magnitudes in excess of 4 km/s. From 71° INV to 68° INV a narrow zone of westward flow occurs with magnitudes similar to the polar cap flow. Equatorward of 68° INV a region of weaker flow is evident with an average antisunward direction. On this pass the velocity field rotates nearly 90° in one spin (11 s) at 71° INV between the two zones of intense flow.

Differential electron intensities for this pass are plotted in the lower two panels of Figure 3 for 180 eV and 5.2 keV. The electron flux for energies greater than 45 keV is plotted in the top panel. The 180-eV electron fluxes indicate a narrow intense event at 2053:25 UT and a broader peak at 2055:00 UT. The 5.2-keV record shows no fluxes above threshold before 2054:50 UT. A small peak occurs at 2055:00 UT coincident with a distinct intensity maximum at 180 eV, and at 2056:00 UT the flux rises above threshold for the remainder of the pass. The flux of electrons with energies greater than 45 keV is always above threshold except for the first 20 s of this pass. A gradual increase in the $E_e > 45$ keV electron intensities occurs between 2053:30 UT and 2056:00 UT. At 2056:00 UT the $E_e > 45$ keV intensities suddenly increase to 6×10^5 electrons $(\text{cm}^2\ \text{s}\ \text{sr})^{-1}$ followed by a slow increase until 2100:00 UT. The location of the electric field reversal is indicated by a vertical line at 2255:35. Since the reversal occurs in one spin, the temporal resolution for the electric field reversal determination is ±6 s. The reversal separates the 180-eV fluxes over the polar cap from the equatorward 5.2-keV fluxes associated with the outer zone.

To identify the origin of the intense 180-eV fluxes, two particle spectra are shown in Figure 4 from measurements made at 2053:25 UT and 2054:45 UT. Both spectra show a peak near 200 eV, which is consistent with a magnetosheath

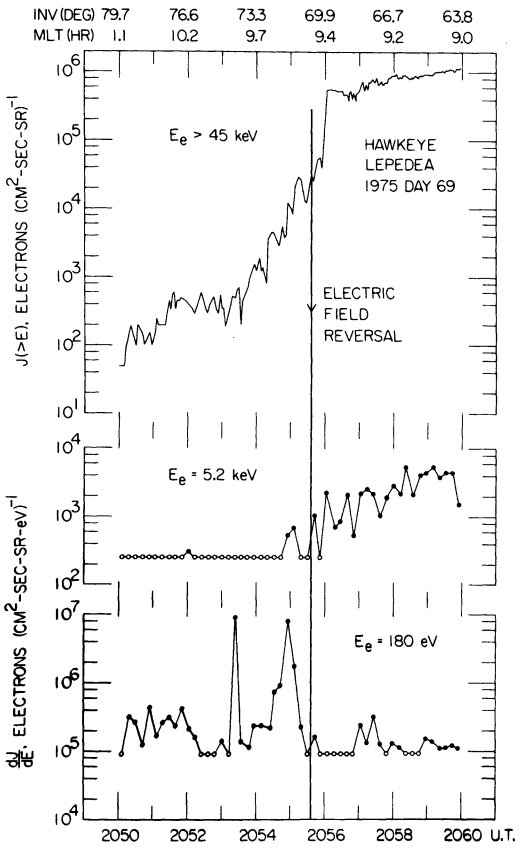

Fig. 3. Electron fluxes for $E_e > 45$ keV (top panel), $E_e = 5.2$ keV (middle panel), and $E_e = 180$ eV (bottom panel) for the pass shown in Figure 2. The vertical line is the position of the electric field reversal. Note the abrupt onset of the 5.2-keV electron intensities at the electric field reversal and the low-energy, ~180 eV, electrons poleward of the electric field reversal.

origin for these particles. Pitch angles change rapidly while the energy spectrum is measured, and the range of pitch angles is indicated on each plot. Since the loss cone is 32°, only the very low energies at 2054:45 UT represent electrons which could possibly be arriving from the ionosphere.

The convection velocity measurements for day 263, September 20, 1974, are shown in Figure 5. The plasma flow over the polar cap during this pass is primarily east-west, but two distinct zones of sunward and antisunward convection are apparent. From 83° INV to 76° INV, plasma flows toward the east with a small component in the antisunward direction. The flow reverses, within one spin of the spacecraft, at 76° latitude, followed by westward flow with a component in the sunward direction until 67° INV. Equatorward of this point the convection velocity is less than 1 km/s in the antisunward direction.

For this pass, Figure 6 shows the differential electron intensities at 180 eV and 5.2 keV in the lower two panels and the integral electron intensity above 45 keV in the upper panel. The fluxes of electrons greater than 45 keV begin to decrease at 2242 UT and continue to decrease until 2245 UT. A solar proton event during this period maintains the count rate at an equivalent intensity of 4×10^3 electrons $(\text{cm}^2\ \text{s}\ \text{sr})^{-1}$ The differential electron intensities at 5.2 keV gradually increase until 2244 UT and then decline to values corresponding to threshold at 2244:30 UT for the remainder of the pass. Between 2237 UT and 2242 UT the electron intensities at 180 eV slowly decrease to threshold intensities. At 2243 UT the 180-eV fluxes suddenly increase and remain elevated to at least 2246 UT. The average flux is about 5×10^5 electrons $(\text{cm}^2\ \text{s}\ \text{sr}\ \text{eV})^{-1}$, which is consistent with previous observations in the polar cusp. The electric field reverses within one spin period, and the time of the reversal is shown as a vertical line. On this pass the electric field reversal marks the trapping boundary for 5.2 keV electrons, while the 180-eV electron intensities are located within 5° of latitude on either side of the reversal.

Two electron spectra are presented in Figure 7 for periods during the intense 180-eV electron fluxes but on either side of the reversal. Above 1 keV the differential fluxes decrease as the spacecraft passes poleward of the electric field reversal. Below 1 keV and equatorward of the reversal, peaks in the spectrum are observed between 500 eV and 1 keV and between 100 and 200 eV. The spectral peaks are also observed poleward of the reversal, and in this case their relative intensities are reversed. The electron differential intensities below 1 keV for these cases

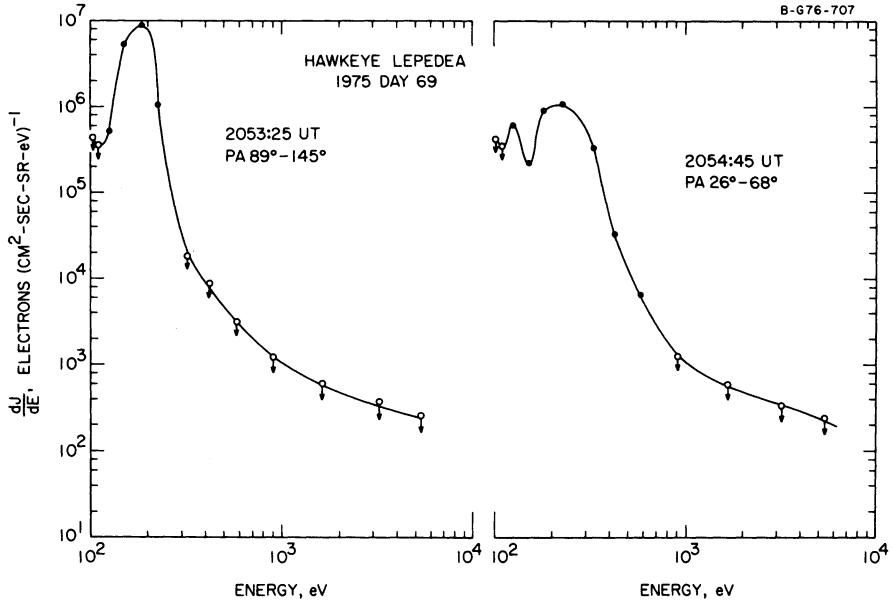

Fig. 4. Electron energy spectra for March 10, 1975. The indicated pitch angle range corresponds to the pitch angles at the beginning and end of each spectrum.

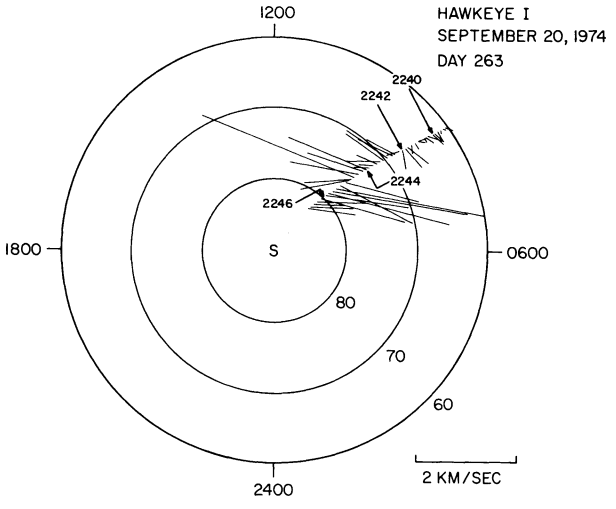

Fig. 5. The **E** × **B** velocities for a pass over the southern polar cap on September 20, 1974.

are similar to those of the magnetosheath, although those for 2243:30 UT are somewhat lower than those usually found in the magnetosheath proper.

Discussion

The term polar cusp in most cases refers to a particular plasma distribution found at high latitudes which resembles the plasma found in the magnetosheath. The proton spectrum peaks between 1 and 2 keV. Electrons peak at energies less than 1 keV, usually between 100 and 200 eV, with typical fluxes of 10^6–10^7 electrons $(cm^2\ s\ sr\ eV)^{-1}$. At low altitudes this plasma signature is usually located within a strip between 70° and 85° invariant latitude and extending from 0800 to 1600 MLT. The latitudinal width of the strip has been reported as small as 0.2° INV latitude and as large as 6° INV latitude. For the remainder of this discussion we will assume that there exists a distribution of plasma over the ionosphere with the above characteristics and that the low-energy electron records presented here measure the spatial extent of the cusp along the Hawkeye 1 orbit near 2000-km altitude. We have restricted ourselves to electron measurements, since the threshold for the rapid scan proton channel at 2 keV is 10^3 protons $(cm^2\ s\ sr\ eV)^{-1}$, which is too large for typical proton intensities in the cusp to be detected. These proton intensities are surveyed with the slower digital accumulator section of the instrument.

For the two satellite passes presented here the electric field changes within one rotation period of the spacecraft or within 0.5° of INV latitude. This sharp boundary has been reported by both *Cauffman and Gurnett* [1971] and *Heppner* [1972*b*]. *Heelis et al.* [1976] have further resolved the polar velocity field, using ion drift detectors which indicate that there is a narrow region near noon in which the plasma flows across the polar cusp boundary. The velocity rotation on day 69 apparently is of this type.

The 5.2-keV electron population is observed on dayside field lines equatorward of the electric field reversal and the cusp. This population probably originates near the inner edge of the plasma sheet, then gradient drifts toward morning and convects sunward. These electrons are located inside the magnetosphere, and their poleward boundary is within 1° (slightly equatorward) of the electric field reversal for both cases presented here. The close agreement of these two boundaries implies that the 5.2-keV electron intensities fall below the detector threshold because they are no longer durably trapped. Hence the 5.2-keV electron threshold boundary supports the premise that the poleward boundary of closed dayside field lines does not lie equatorward of the electric field reversal.

The $E_e > 45$ keV electron flux begins to decrease in both cases at a latitude equatorward of the cusp and electric field reversal. A solar proton event on day 263 prevents the Geiger tube from reaching threshold and maintains an equivalent background intensity of 4×10^3 electrons $(cm^2\ s\ sr)^{-1}$ over the polar cap. On day 69 the $E_e > 45$ keV flux is at the threshold of 50 electrons $(cm^2\ s\ sr)^{-1}$ only briefly at the beginning of the record in a region 10° poleward of the electric field reversal. *Frank* [1965], using a similar instrument at high altitudes in the morning sector, observes no clear cutoff of $E_e > 45$ keV electron intensities at altitudes beyond 15 R_E within 30° of the equatorial plane. *Winningham* [1972] has found $E_e > 45$ keV electron fluxes inside the cusp at low altitudes, and *McDiarmid et al.* [1976] report seeing the polar cusp entirely equatorward of their instrumental threshold boundary for 40-keV electrons. At most the $E_e > 45$ keV intensity profile restricts the trapping boundary to be located somewhere in the region of the intensity gradient. This is consistent with the electric field and 5.2-keV electron observations.

On day 69 the cusp is located just poleward of the electric field reversal. This agrees with any model where magnetosheath plasma flows down to the ionosphere on field lines threading the magnetosheath or boundary layer. The observed width of the cusp is about 1° of invariant latitude which agrees with the estimate *Frank* [1971] makes at higher altitudes and is smaller than the measurements from Isis 1 at lower altitudes.

The 180-eV electron intensities for day 263 have equatorward and poleward boundaries of 71° INV and 81° INV. A 10° wide cusp is larger than any previously reported. The

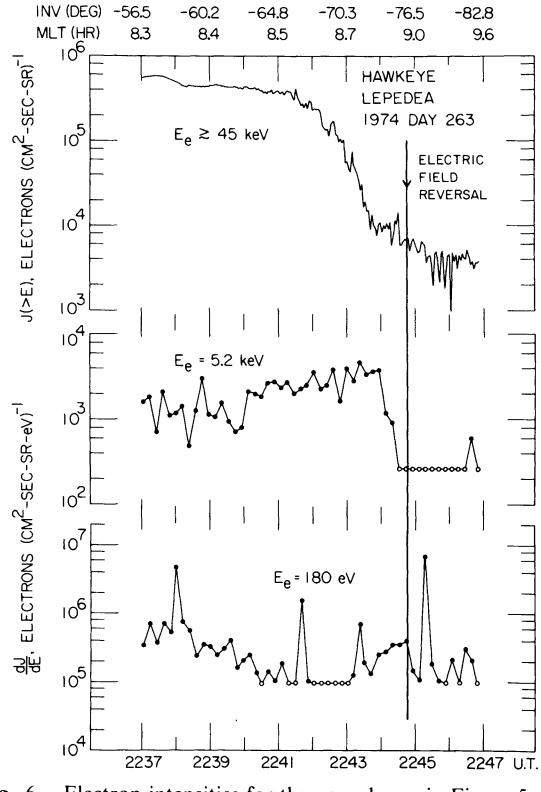

Fig. 6. Electron intensities for the pass shown in Figure 5. Again note the termination of the 5.2-keV electron intensities essentially coincident with the location of the electric field reversal.

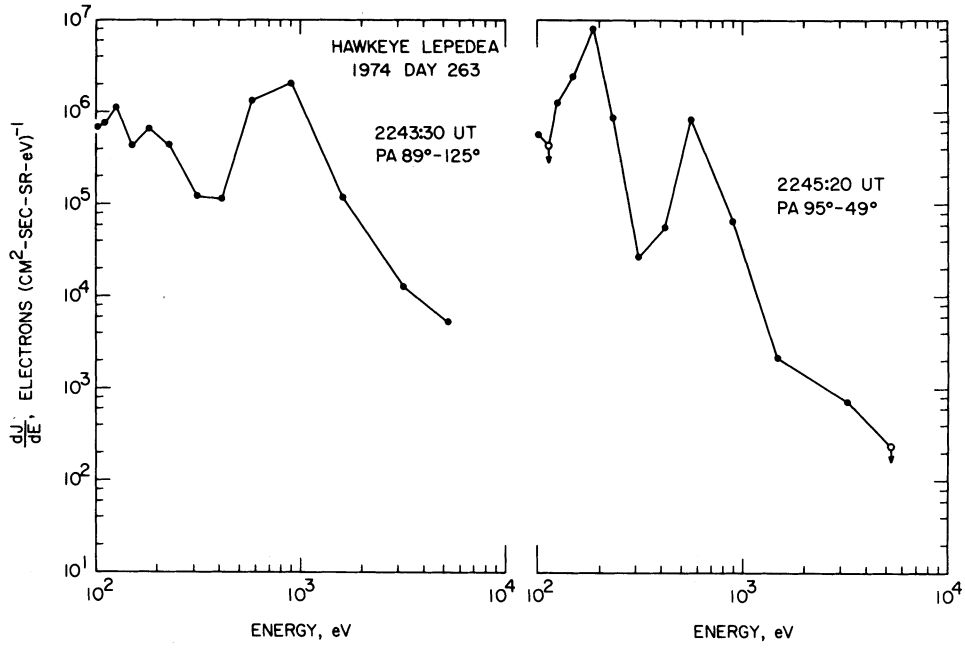

Fig. 7. Electron energy spectra for the pass in Figure 6 equatorward (2243:30 UT) and poleward (2245:20 UT) of the electric field reversal.

poleward boundary of the cusp in this case is not well defined from the electron intensity profiles, and the true width of the cusp may be somewhat smaller. The poleward fluxes may be in part ionospheric projections of the boundary layer [*Ogilvie et al.*, 1971] or of the plasma mantle. Regardless of the correct poleward boundary location the width of this example is several times larger than the previous example and in closer agreement with the results reported from Isis 1 if we use these low-energy electron intensities as sole identification for the polar cusp. Then the equatorward boundary of the cusp lies 5° equatorward of the electric field reversal on field lines populated by 5.2-keV electrons. Clearly, these field lines are closed dayside field lines.

Equatorward of the electric field reversal the 180-eV electron intensities are more uniform than those poleward of the reversal. The single intense peak at 2245:15 has a maximum width of 60 km in the lower ionosphere. Similarly narrow events have been observed at sounding rocket altitudes by *Maynard and Johnstone* [1974].

D'Angelo [1973] shows that earthward streaming protons in the cusp are susceptible to the Kelvin-Helmholtz instability. The resulting turbulence enhances cross-field diffusion and is capable of transporting protons across 2° of latitude at the Bohm diffusion rate. Electrons may diffuse somewhat faster if they are not inhibited by ambipolar forces. The distribution on day 263 is located 5° equatorward of the electric field reversal and does not decay from a source, as would be expected for cross-field diffusion. This mechanism may contribute to transporting cusp plasma onto closed field lines, but it does not appear to be the dominant process on day 263.

Paschmann et al. [1976] have investigated the polar cusp near the magnetosheath, using particle detectors and magnetometers. They find that on closed dayside magnetic field lines, equatorward of the estimated neutral line and adjacent to the magnetosheath, there exists a region of plasma with density and temperature equal to the density and temperature of the magnetosheath but with variable flow velocity and direction; they call this region the entry layer. The first example they present has a narrow inner boundary and is sufficiently wide to project into the area of low-energy electrons observed equatorward of the electric field reversal on day 263. This single example is not conclusive, but it is consistent with the interpretation that the low-energy electrons on closed field lines during day 263 are the low-altitude projection of the entry layer.

CONCLUSIONS

The two examples presented here are insufficient to make a general statement on the relative locations of the trapping boundary, the electric field reversal, and the low-altitude cusp, but they do prescribe a minimum range of relative positions for these structures.

In both cases the electric field reversal occurs within 1° of invariant latitude poleward of the termination of measurable 5.2-keV electron intensities, and these two structures occur poleward of the intitial 45-keV electron flux decrease. The electric field reversal probably represents the boundary between closed dayside field lines and field lines threading the magnetosheath, the boundary layer, or the tail.

Electrons of magnetosheath origin populate field lines just poleward of the electric field reversal and in some cases populate field lines equatorward of the electric field reversal. The width of the cusp varies from 1° to at least 6° of latitude at 2000-km altitude. The equatorward low-energy electron population on day 263 may be an extension of the entry layer reported by *Paschmann et al.* [1976] to low altitudes.

The equatorward boundary of the low-energy electron distribution does not always coincide with the low-latitude boundary of the polar cap. We caution against interpreting the equatorward termination of low-energy electron intensities as the boundary between closed dayside field lines and polar cap field lines.

Acknowledgments. The authors wish to thank R. West for programing assistance with the electric field data. This research was supported in part by the National Aeronautics and Space Administration under grants NGL-16-001-043 and NGL-16-001-002 and contract NAS1-13129 and by the Office of Naval Research.

The Editor thanks W. Heikkila for his assistance in evaluating this paper.

REFERENCES

Akasofu, S.-I., Midday auroras and magnetospheric substorms, *J. Geophys. Res., 77*, 244, 1972*a*.

Akasofu, S.-I., Midday auroras at the south pole during magnetospheric substorms, *J. Geophys. Res., 77*, 2303, 1972*b*.

Cain, J. C., and R. A. Langel, The geomagnetic survey by the polar orbiting geophysical observatories Ogo-2 and Ogo-4 1965–1967, *Rep. X-612-68-502*, Goddard Space Flight Center, Greenbelt, Md., 1968.

Cauffman, D. P., and D. A. Gurnett, Double-probe measurements of convection electric fields with the Injun 5 satellite, *J. Geophys. Res., 76*, 6014, 1971.

D'Angelo, N., VLF fluctuations at the polar cusp boundaries, *J. Geophys. Res., 78*, 1206, 1973.

Frank, L. A., A survey of electrons $E > 40$ keV beyond 5 earth radii with Explorer 14, *J. Geophys. Res., 70*, 1593, 1965.

Frank, L. A., Plasma in the earth's polar magnetosphere, *J. Geophys. Res., 76*, 5202, 1971.

Frank, L. A., and K. L. Ackerson, Observations of charged particle precipitation into the auroral zone, *J. Geophys. Res., 76*, 3612, 1971.

Gurnett, D. A., and L. A. Frank, Observed relationships between electric fields and auroral particle precipitation, *J. Geophys. Res., 78*, 145, 1973.

Heelis, R. A., W. B. Hanson, and J. L. Burch, Ion convection velocity reversals in the dayside cleft, *J. Geophys. Res., 81*, 3803, 1976.

Heikkila, W. J., and J. D. Winningham, Penetration of magnetosheath plasma to low altitudes through the dayside magnetospheric cusp, *J. Geophys. Res., 76*, 883, 1971.

Heikkila, W. J., J. D. Winningham, R. H. Eather, and S.-I. Akasofu, Auroral emissions and particle precipitation in the noon sector, *J. Geophys. Res., 77*, 4100, 1972.

Heppner, J. P., Polar-cap electric field distributions related to the interplanetary magnetic field direction, *J. Geophys. Res., 77*, 4877, 1972*a*.

Heppner, J. P., Electric field variations during substorms: Ogo-6 measurements, *Planet. Space Sci., 20*, 1475, 1972*b*.

Kivelson, M. G., C. T. Russell, M. Neugebauer, F. L. Scarf, and R. W. Fredricks, Dependence of the polar cusp on the north-south component of the interplanetary magnetic field, *J. Geophys. Res., 78*, 3761, 1973.

Maynard, N. C., and A. D. Johnstone, High-latitude dayside electric field and particle measurements, *J. Geophys. Res., 79*, 3111, 1974.

McDiarmid, I. B., J. R. Burrows, and E. E. Budzinski, Particle properties in the dayside cleft, *J. Geophys. Res., 81*, 221, 1976.

Ogilvie, K. W., J. D. Scudder, and M. Sugiura, Magnetic field and electron observations near the dawn magnetosphere, *J. Geophys. Res., 76*, 3574, 1971.

Paschmann, G., G. Haerendel, N. Sckopke, H. Rosenbauer, and P. C. Hedgecock, Plasma and magnetic field characteristics of the distant polar cusp near local noon: The entry layer, *J. Geophys. Res., 81*, 2883, 1976.

Russell, C. T., C. R. Chappell, M. D. Montgomery, M. Neugebauer, and F. L. Scarf, Ogo 5 observations of the polar cusp on November 1, 1968, *J. Geophys. Res., 76*, 6743, 1971.

Wescott, M. E., J. D. Stolarik, and J. P. Heppner, Electric fields in the vicinity of auroral forms from motions of barium vapor releases, *J. Geophys. Res., 74*, 3469, 1969.

Winningham, J. D., Characteristics of magnetosheath plasma observed at low altitudes in the dayside magnetospheric cusps, in *Earth's Magnetospheric Processes*, edited by B. M. McCormac, D. Reidel, Hingham, Mass., 1972.

Yasuhara, F., S.-I. Akasofu, J. D. Winningham, and W. J. Heikkila, Equatorward shift of the cleft during magnetospheric substorms as observed by Isis I, *J. Geophys. Res., 78*, 7286, 1973.

(Received January 24, 1977;
accepted June 15, 1977.)